論文 / 著書情報
Article / Book Information

Title	Low-loss waveguide optical isolator with tapered mode converter and magneto-optical phase shifter for TE mode input
Authors	Ryusuke Yamaguchi, Yuya Shoji, Tetsuya Mizumoto
Citation	Optics Express, Vol. 26, No. 16, pp. 21271-21278
Pub. date	2018, 8
Copyright	(c) 2018 Optical Society of America. Users may use, reuse, and build upon the article, or use the article for text or data mining, so long as such uses are for non-commercial purposes and appropriate attribution is maintained. All other rights are reserved.
DOI	http://dx.doi.org/10.1364/OE.26.021271

Research Article | Vol. 26, No. 16 | 6 Aug 2018 | OPTICS EXPRESS 21271
Optics EXPRESS

Low-loss waveguide optical isolator with tapered mode converter and magneto-optical phase shifter for TE mode input

RYUSUKE YAMAGUCHI,[1] YUYA SHOJI,[1,2,*] AND TETSUYA MIZUMOTO[1,2]

[1]*Department of Electrical and Electronic Engineering, Tokyo Institute of Technology, 2-12-1Ookayama, Meguro-ku, Tokyo 152-8552, Japan*
[2]*Laboratory for Future Interdisciplinary Research of Science and Technology, Tokyo Institute of Technology, 2-12-1 Ookayama, Meguro-ku, Tokyo 152-8552, Japan*
**shoji@ee.e.titech.ac.jp*

Abstract: We propose and demonstrate a novel low-loss waveguide optical isolator with tapered mode converter and magneto-optical phase shifter. The principle of operation of the isolator is based on the superposition of the TE and TM modes. The two different modes become direction-dependent due to a magneto-optical phase shift affecting the TM mode. We designed a tapered mode converter in order to generate the TE and TM modes with equal amplitude when the waveguide is excited with a TE mode input. We successfully demonstrated that the fabricated device acts as an isolator showing a different transmittance between forward and backward directions. The maximum isolation measured is 16 dB at a wavelength of 1561 nm for a TE mode input.

1. Introduction

Semiconductor lasers and semiconductor optical amplifiers are widely used in optical fiber communication systems. When backward reflections are launched into these devices, their performance degrades, becoming afflicted by instability due to intensity and phase noises. To avoid these problems, optical isolators that allow one-way lightwave transmission are installed, along with active optical devices, in the optical fiber communication systems. Bulk-type optical isolators are commercially available and still widely used, but they are difficult to integrate with optical active devices.

Silicon photonic waveguides on a silicon-on-insulator (SOI) wafer are useful for constructing photonic integrated circuits (PICs) with small footprints. Waveguide optical isolators are highly demanded for silicon PICs. Strict optical isolation, independent of light intensity, has been realized with both electro-optical and magneto-optical effects. Electro-optical types use dynamic optical modulators which can be fabricated with CMOS compatible processes. However, they can cause additional losses and power consumption [1–3]. On the other hand, magneto-optical materials are not compatible with silicon. Magnetic metals are lossy and growth of magneto-optical garnet on silicon is still challenging [4,5]. So far, magneto-optical isolators fabricated by direct bonding technology have been realized with superior performance [6–11]. These isolators are configured as Mach-Zehnder interferometers (MZI) or ring resonators. They work with a fundamental TM mode input since the non-reciprocal function is provided by a magneto-optical phase shift that occurs only for TM modes propagating in a silicon waveguide with a bonded garnet upper cladding layer. On the other hand, most optical active devices operate in the TE mode. In order to realize the desired magneto-optical phase shift while having a TE mode input, a lateral asymmetry in waveguide structure is needed. This makes the fabrication process rather complicated. Waveguide integrated TE-TM mode converters with magneto-optical TM mode isolator represent a straightforward approach to the realization of optical isolators that work with TE mode input [6,10].

#334495 https://doi.org/10.1364/OE.26.021271
Journal © 2018 Received 5 Jun 2018; revised 22 Jul 2018; accepted 26 Jul 2018; published 2 Aug 2018

Optics EXPRESS

In this article, we propose a novel waveguide optical isolator with incorporated TE-TM half mode converters and a magneto-optical phase shifter for the TM mode. Optical isolation is achieved via a phase difference between reciprocal TE and nonreciprocal TM propagations. Thanks to the new configuration, scattering loss at the magneto-optical garnet boundaries can be reduced. Moreover, our proposed configuration needs simply an external, one directional applied magnetic field rather than the anti-parallel or radial one needed for MZI or ring resonator configurations. Consequently, the device has both simple structure and small footprint. We also designed and implemented a tapered TE-TM half mode converter. Finally, we fabricated the proposed optical isolator and demonstrated optical isolation along with low insertion loss.

2. Operation principle

The schematic of the proposed optical isolator is shown in Fig. 1. It consists of two tapered TE-TM mode converters and a magneto-optical phase shifter. The device operation is based on the interference between the TE and TM modes propagating in the magneto-optical phase shifter, the upper cladding layer of which consists of a magneto-optical garnet. In the magneto-optical phase shifter of the proposed device, an external magnetic field is applied in only one direction, whereas it is applied in anti-parallel directions in other previous MZI devices. This can reduce the device footprint and allows denser integration. The tapered TE-TM mode converter works as a 3 dB power divider and as a combiner of TE and TM modes mediated by higher TE modes. The input and output light show both a TE field configuration It provides one-way light propagation using nonreciprocal phase shift for the TM mode.

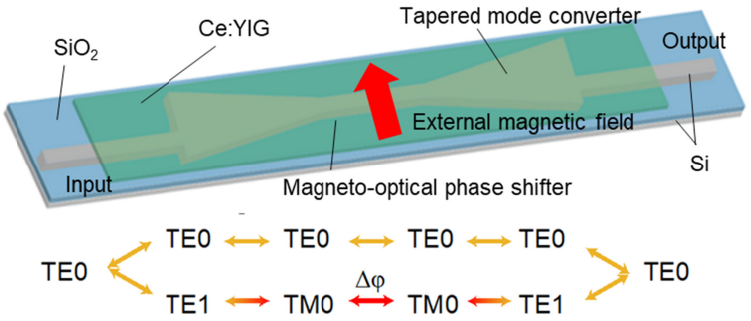

Fig. 1. Structure of the proposed waveguide optical isolator. Ce:YIG is directly bonded on a Si waveguide as an upper cladding layer and magnetized in the film plane by an external magnetic field. Lower shows mode excitation and transition inside the device.

The structure of the tapered TE-TM mode converter is shown in Fig. 2(a). We show how to design the dimensional parameters of the tapered mode converter in Section 3.1. The design principle is herein explained. An input waveguide is connected to the tapered mode converter so that the launched TE_0 mode light is converted into TE_0 and TE_1 modes with equal amplitude at the interface of the narrow and wide waveguides. This is similar to what happens in a multimode interference (MMI) coupler. Hereafter we call this interface an MMI junction. It is known that mode conversion occurs between the TE_1 and TM_0 when the effective refractive indices match each other in a vertically asymmetric waveguide where the refractive indices of the upper and lower cladding layers are different [12]. This mode conversion occurs adiabatically in a tapered region around the index-matching point. Figure 2(b) shows that the TM_0 mode is generated while the electromagnetic field is propagating in the tapered structure. In order to expand the region in which this modal conversion happens efficiently, we use a three-step taper. In this way, the input fundamental TE_0 mode is converted into TE_0 and TM_0 modes with equal amplitude.

Optics EXPRESS

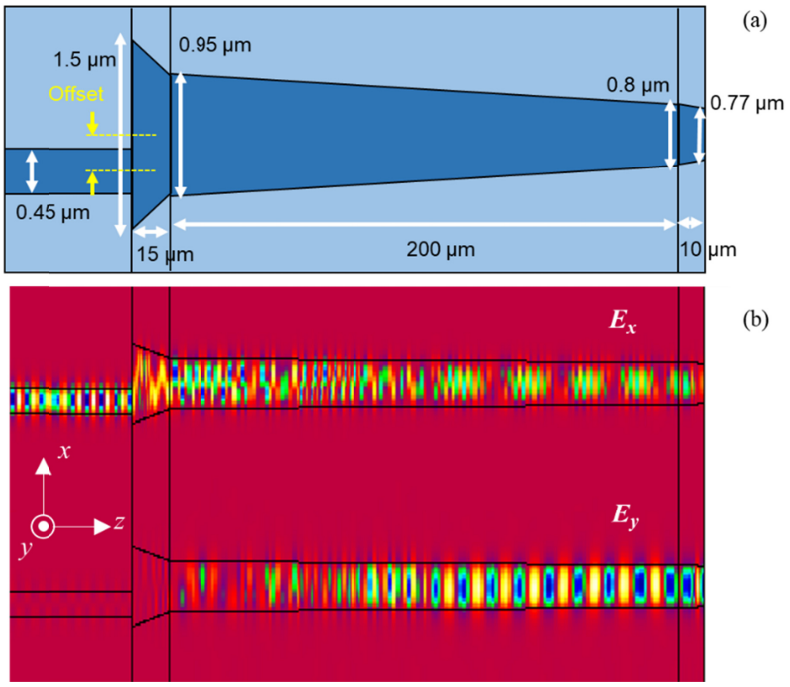

Fig. 2. (a) Top view of Si waveguide structure of the tapered mode converter. (b)Power distribution of E_x, and E_y for TE_0 mode input. In the tapered middle section, multi-mode interference between TE_0 and TE_1 modes is observed for E_x, while the TE_1 mode is gradually converted into TM_0 mode via a hybrid mode.

The magneto-optical phase shifter is composed of a Si waveguide with an upper cladding layer of magneto-optical garnet $CeY_2Fe_5O_{12}$ (Ce:YIG) which has a Faraday rotation coefficient of –4500 °/cm [13,14]. Since the waveguide is asymmetric in the vertical direction, a magneto-optical phase shift is generated for the TM modes when an external magnetic field is applied in the film plane [15]. The TE_0 and TM_0 modes propagate independently in the waveguide, but the TM_0 mode experiences a magneto-optical phase shift. We adjust the propagation distance of the magneto-optical phase shifter so that the TE_0 and TM_0 modes are respectively in-phase and out-of-phase in the forward and backward directions.

In the forward direction, TE mode input light is converted within the input tapered TE-TM mode converter into TE_0 and TM_0 modes with an equal amplitude. After propagating in the magneto-optical phase shifter, the two modes become in phase. In the output tapered TE-TM mode converter, TM_0 mode is re-converted into TE_1 mode, and then the TE_0 and TE_1 interfere constructively at the output MMI junction. They are finally coupled to the output waveguide as a TE mode as shown in Fig. 3(a). In the backward direction, TE mode light launched from the output waveguide is converted in the tapered TE-TM mode converter into TE_0 and TM_0 modes. In this direction, a π phase difference is introduced between TE_0 and TM_0 modes after propagating in the magneto-optical phase shifter due to the nonreciprocal phase shift affecting the TM mode. The TE_1 mode resulting from the conversion of the TM_0 mode is phase shifted in respect to the TE_0 mode by π, TE_0 and TE_1 modes interfere destructively at the MMI junction. Therefore, in the backward direction, the input TE mode light is not coupled to the input port, but is scattered at the MMI junction as shown in Fig. 3(b). In this way, the characteristic modus operandi of an isolator is achieved.

Optics EXPRESS

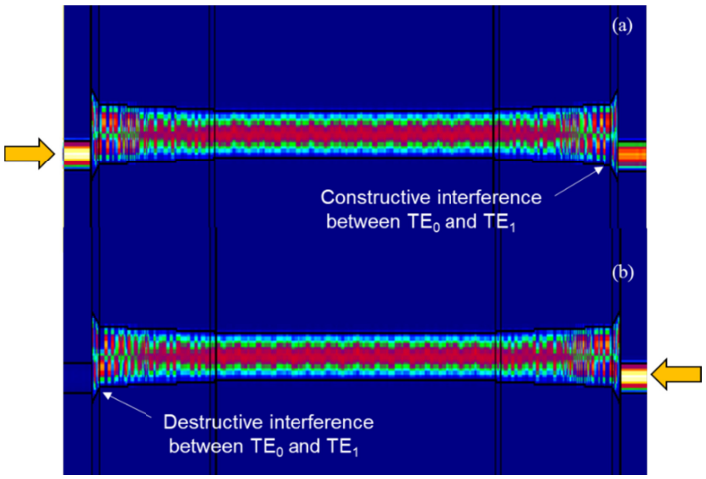

Fig. 3. Power distribution in case of (a) in-phase interference in the forward direction and (b) out-of-phase interference in the backward direction.

3. Design and fabrication

3.1 Design

We designed the MMI junction so that the TE_0 and the TE_1 modes could be excited with an equal amplitude. The power ratio of the two modes depends on the position of the input waveguide relative to the MMI junction. Figure 4 shows how the excited mode ratio depends on the offset between the center of the tapered waveguide and that of the narrow waveguide connected to the taper. The widths of the narrow waveguide and the taper end are respectively 0.5 μm and 1.5 μm. Figure 4 also shows that the power of the TE_0 and the TE_1 modes become equal when the offset is 0.335 μm. Although the TE_2 mode is excited at the junction, we adopted a width of 1.5 μm at the taper end in view of the possibility to include the design an optical circulator.

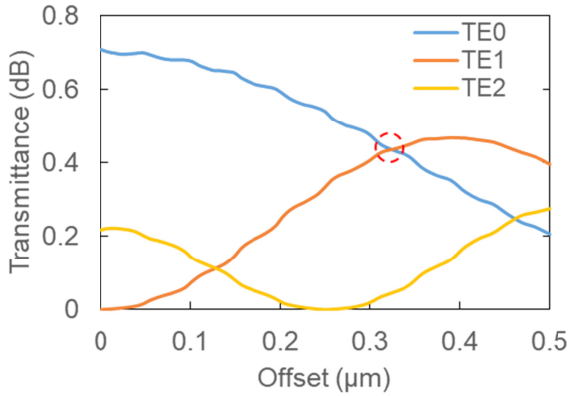

Fig. 4. Conversion ratio at MMI junction as a function of offset. Offset of zero corresponds to the case that the narrow input waveguide is coaxially connected to the wide MMI section.

Figure 5(a) shows calculated effective refractive indices of propagation mode as a function of waveguide width. The index matching between the TE_1 and TM_0 modes occurs when the waveguide is 0.85-μm wide. Figure 5(b) shows calculated transmittance of the TE_0 and TM_0 modes in the tapered middle section. The length of the tapered middle section of the waveguide is 200 μm because a gradual change in width is needed in order to have enough

Optics EXPRESS

TE-TM mode conversion. TE_1 mode light at the 1.5-μm-wide waveguide is efficiently converted into the TM_0 mode at the end of the tapered waveguide.

The thickness of Si waveguide is chosen to be 220 nm in order to obtain maximum magneto-optical phase shift, which contributes to reducing the footprint of the device. Figure 6 shows the magneto-optical phase shift calculated at a wavelength of 1550 nm as a function of waveguide width. The waveguide width of magneto-optical phase shifter is 0.77 μm because the wider waveguide provides larger magneto-optical phase shift, while it is less than 0.85 μm in order to achieve the best compromise with TE-TM mode converter. The length required for a phase difference of π between the forward and backward TM_0 modes is calculated to be 520 μm for the 770-nm-wide Si waveguide at a wavelength of 1550 nm.

Let us mention the robustness of this device with respect to fabrication variability on a scale of several tens nanometer. A change in TE-TM mode conversion efficiency is negligible owing to the tapered structure. The excitation ratio of TE_0 and TE_1 modes is dominated by the offset of input waveguide. The magneto-optical phase shift is also robust against a change in waveguide width. The operation bandwidth, determined by the difference in a propagation constant between TE_0 and TM_0 modes, is insensitive to such a dimensional change because changes in two modes are almost equal. Since the absolute phase of propagating light is hardly determined in the Si photonic waveguides, a thermal tuning is useful to control the central operating wavelength.

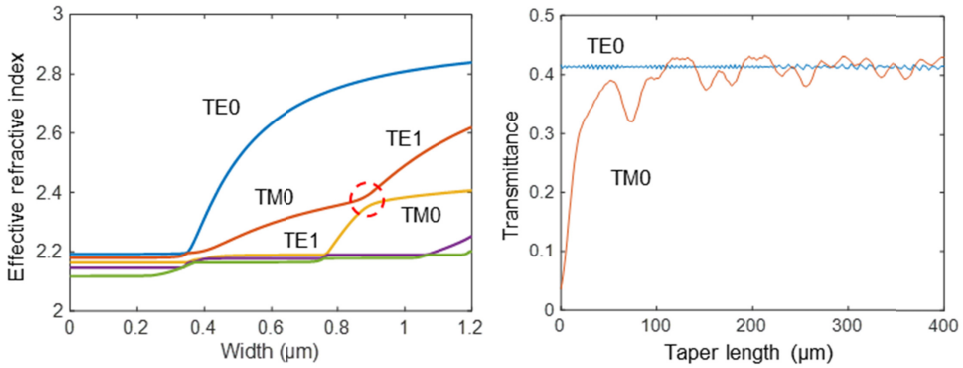

Fig. 5. (a)Dependence of effective indices of Si waveguide with a Ce:YIG cladding layer. (b)The taper length dependence of modal power for TE_0 and TM_0 modes propagating in the tapered middle section of TE-TM mode converter.

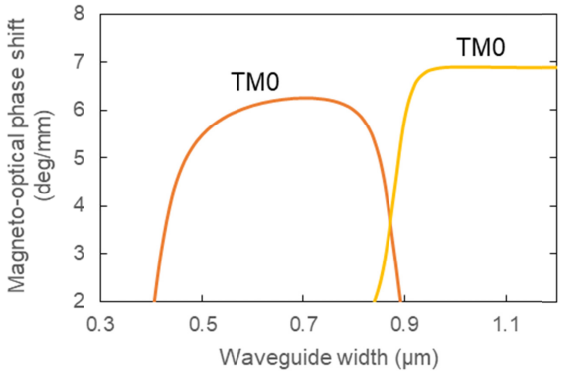

Fig. 6. Magneto-optical phase shift of TM_0 mode calculated at a wavelength of 1550 nm as a function of silicon waveguide width. Two curves correspond to the electromagnetic fields of propagation mode shown by the respective color in Fig. 5(a).

Optics EXPRESS

3.2 Fabrication

The waveguide was formed in a 220-nm thick Si layer on a SOI wafer using electron-beam lithography followed by a SF_6 reactive ion etching with SiO_2 mask. A 500-nm-thick single-crystalline Ce:YIG layer grown on a SGGG substrate was directly bonded on a silicon waveguide using a surface activated direct bonding technique. We applied pressure of 12 MPa at the temperature of 200 °C in the bonding process. Due to our limited wafer manipulation capability, we used a 1500-μm-square Ce:YIG die, which was large enough to cover the whole device. Figure 7 shows a microscopic image of the fabricated isolator.

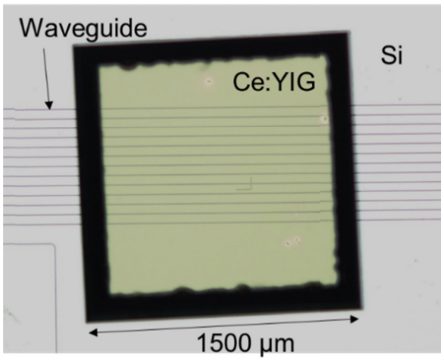

Fig. 7. Microscopic image of the fabricated isolator. 1500-μm-square Ce:YIG/SGGG die was directly bonded on Si waveguides.

4. Characterization

The transmittance of the fabricated device was measured using a fiber-device-fiber setup. TE-polarized light from an amplified spontaneous emission light source was launched into our device through a focusing lens module with a polarizer. The light transmitted through the device was coupled to an output optical fiber by another focusing lens module with a polarizer. The fiber-to-fiber transmittance was measured using a spectrum analyzer. An external magnetic field of ~100 Oe was applied to the Ce:YIG layer transversally to the propagation direction in the film plane via a two poles permanent magnet located above the device. The magnetic field direction was reversed by inverting the permanent magnet. Reversing the direction of the magnetic field applied to the Ce:YIG layer reverses the propagation direction because of the symmetry of the device. Hereafter we call these two situations forward and backward propagations respectively.

Figure 8 shows the measured transmission spectra of TE mode. The coupling losses between the input and output lens modules and the device are included in the measured transmittance. The blue and red lines show the forward and backward transmittances, respectively. The TM_0 mode converted from the TE_1 mode is propagated in the magneto-optical phase shifter with a different propagation constant from the one characterizing the TE_0 mode. The interference between TE_0 and TE_1 modes was observed in the transmitted output.

When an external magnetic field is applied, different transmittances are observed depending on the direction of propagation. An applied magnetic field causes a magneto-optical phase shift in the TM mode. The propagation constant of the TM mode is slightly higher in the forward propagation in comparison to the non-magnetized case. The TE mode is not affected by the magneto-optical effect. Because of this, the interference spectrum is blue-shifted. When the propagation direction is reversed, the magneto-optical phase shift changes its sign. In this case, the propagation constant is slightly less than in the non-magnetized case. This, in turn, results in a red shift of the spectrum. As a result, different transmittances are observed depending on the propagation direction. The fringe present in the spectra was induced by Fabry-Perot resonance between the input and output MMI junctions. The actual

Optics EXPRESS

transmittance level would be the middle between the top and bottom of the fringe in a linear scale. For example, an actual backward transmittance is estimated to be −53.6 dB at a wavelength of 1561 nm. An isolation ratio of 16 dB, which is defined by the ratio of the forward to the backward transmittance, is obtained at this wavelength. The isolation bandwidth is determined by the free-spectral range due to TE and TM mode phase difference.

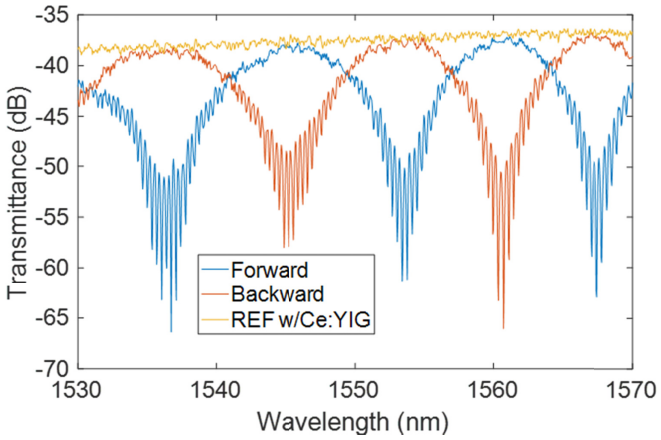

Fig. 8. Measured transmittance spectra of our fabricated optical isolator. Blue and red lines are the transmittances of the isolator for forward and backward directions, respectively. Orange line is the transmittance of the reference waveguide with a Ce:YIG upper cladding layer.

The orange line in Fig. 8 shows the transmittance of the reference waveguide adjacent to the isolator where a Ce:YIG upper cladding layer is bonded. Although the transmittance of a waveguide without a Ce:YIG upper cladding layer is not shown, it was at the same level of the one we measured on our device or worse. This means that the insertion loss of this device was considerably small. The previously reported MZI optical isolator has a large insertion loss of ~13 dB [7]. The loss is due to mode mismatch at the interface between the air cladding and the Ce:YIG cladding waveguides and optical absorption of the TM mode in the Ce:YIG cladding layer. On the other hand, losses associated with mode mismatch and optical absorption are smaller for the TE mode in comparison to the TM mode, because the TE mode is better confined in the waveguide than the TM mode. We simulated loss due to the mode mismatch and the optical absorption of Ce:YIG for the TE and TM modes at a wavelength of 1550 nm. The mode mismatch loss was calculated by eigen-mode expansion method. The absorption loss was calculated with a Ce:YIG material loss of ~5 dB/mm and a confinement factor multiplied by the propagation length. Table 1 summarized the loss breakdown of MZI and proposed configurations. The simulation results show lower insertion loss of the proposed configuration compared with the MZI isolator. The proposed optical isolator keeps the TM mode to the minimum necessary. The TE mode propagates across the interface between the air cladding and the Ce:YIG cladding waveguides. This opens an avenue for the realization of low loss optical isolators.

Table 1. Simulated loss breakdown of optical isolator

	MZI configuration	Proposed configuration
Mode mismatch loss	4.3 dB × 2 facets (TM_0)	0.19 dB × 2 facets (TE_0)
Absorption loss	3.7 dB/mm × ~1.5 mm (TM_0)	1.2 dB/mm × ~1.0 mm (TE_0) 3.7 dB/mm × ~0.5 mm (TM_0)
Total loss	14.2 dB	3.4 dB

Optics EXPRESS

5. Conclusion

We proposed a novel waveguide optical isolator composed of two tapered TE-TM mode converters and a magneto-optical phase shifter for the TM mode. The device has two main advantages, namely TE mode input operation and ease of magnetization. An optical isolation of 16 dB was demonstrated at a wavelength of 1561 nm for the TE mode input. To obtain higher extinction, splitting ratio of TE to TM mode in the interferometer should be optimized considering their different propagation losses. Very low loss operation was realized because of good light confinement of the TE mode. The Fabry-Perot resonance can be reduced by connecting output ports for radiating light outside the device in order to prevent the destructive interference.

Funding

JST Core Research for Evolutional Science and Technology (CREST) #JPMJCR15N6; MIC/SCOPE #162103103.

References

1. Z. Yu and S. Fan, "Complete optical isolation created by indirect interband photonic transitions," Nat. Photonics **3**(2), 91–94 (2009).
2. H. Lira, Z. Yu, S. Fan, and M. Lipson, "Electrically driven nonreciprocity induced by interband photonic transition on a silicon chip," Phys. Rev. Lett. **109**(3), 033901 (2012).
3. C. R. Doerr, L. Chen, and D. Vermeulen, "Silicon photonics broadband modulation-based isolator," Opt. Express **22**(4), 4493–4498 (2014).
4. L. Bi, J. Hu, P. Jiang, D. H. Kim, G. F. Dionne, L. C. Kimerling, and C. Ross, "On-chip optical isolation in monolithically integrated non-reciprocal optical resonators," Nat. Photonics **5**(12), 758–762 (2011).
5. X. Y. Sun, Q. Du, T. Goto, M. C. Onbasli, D. H. Kim, N. M. Aimon, J. Hu, and C. Ross, "Single-step deposition of cerium-substituted yttrium iron garnet for monolithic on-chip optical isolation," ACS Photonics **2**(7), 856–863 (2015).
6. S. Ghosh, S. Keyvaninia, Y. Shirato, T. Mizumoto, G. Roelkens, and R. Baets, "Optical isolator for TE polarized light realized by adhesive bonding of Ce:YIG on silicon-on-insulator waveguide circuits," IEEE Photonics J. **5**(3), 6601108 (2013).
7. Y. Shoji and T. Mizumoto, "Magneto-optical non-reciprocal devices in silicon photonics," Sci. Technol. Adv. Mater. **15**(1), 014602 (2014).
8. K. Furuya, T. Nemoto, K. Kato, Y. Shoji, and T. Mizumoto, "Athermal Operation of Waveguide Optical Isolator Based on Canceling Phase deviations in a Mach-Zehnder Interferometer," J. Lightwave Technol. **34**(8), 1699–1705 (2016).
9. D. Huang, P. Pintus, C. Zhang, Y. Shoji, T. Mizumoto, and J. E. Bowers, "Electrically driven and thermally tunable integrated optical isolators for silicon photonics," IEEE J. Sel. Topics Quantum Electron. **22**(6), 4403408 (2016).
10. Y. Shoji, A. Fujie, and T. Mizumoto, "Silicon waveguide optical isolator operating for TE mode input light," IEEE J. Sel. Topics Quantum Electron. **22**(6), 4403307 (2016).
11. P. Pintus, D. Huang, C. Zhang, Y. Shoji, T. Mizumoto, and J. E. Bowers, "Microring-based optical isolator and circulator with integrated electromagnet for silicon photonics," J. Lightwave Technol. **35**(8), 1429–1437 (2017).
12. D. Dai, Y. Tang, and J. E. Bowers, "Mode conversion in tapered submicron silicon ridge optical waveguides," Opt. Express **20**(12), 13425–13439 (2012).
13. M. Gomi, H. Furuyama, and M. Abe, "Strong magneto-optical enhancement in highly Ce-substituted iron garnet films prepared by sputtering," Jpn. J. Appl. Phys. **70**(11), 7065–7067 (1991).
14. T. Shintaku, A. Tate, and S. Mino, "Ce-substituted yttrium iron garnet films prepared on $Gd_3Sc_2Ga_3O_{12}$ garnet substrates by sputter epitaxy," Appl. Phys. Lett. **71**(12), 1640–1642 (1997).
15. H. Dötsch, N. Bahlmann, O. Zhuromskyy, M. Hammer, L. Wilkens, R. Gerhardt, P. Hertel, and A. F. Popkov, "Application of magneto-optical waveguides in integrated optics: review," J. Opt. Soc. Am. B **22**(1), 240–253 (2005).